CO_2 Insulation for Thermal Control of the Mars Science Laboratory

Pradeep Bhandari[1], Paul Karlmann[2], Kevin Anderson[3] and Keith Novak[4]
Jet Propulsion Laboratory, California Institute of Technology, Pasadena, CA 91109

The National Aeronautics and Space Administration (NASA) is sending a large (>850 kg) rover as part of the Mars Science Laboratory (MSL) mission to Mars in 2011. The rover's primary power source is a Multi-Mission Radioisotope Thermoelectric Generator (MMRTG) that generates roughly 2000 W of heat, which is converted to approximately 110 W of electrical power for use by the rover electronics, science instruments, and mechanism actuators. The large rover size and extreme thermal environments (cold and hot) for which the rover is designed for led to a sophisticated thermal control system to keep it within allowable temperature limits. The pre-existing Martian atmosphere of low thermal conductivity CO_2 gas (8 Torr) is used to thermally protect the rover and its components from the extremely cold Martian environment (temperatures as low as -130°C). Conventional vacuum based insulation like Multi Layer Insulation (MLI) is not effective in a gaseous atmosphere, so engineered gaps between the warm rover internal components and the cold rover external structure were employed to implement this thermal isolation. Large gaps would lead to more thermal isolation, but would also require more of the precious volume available within the rover. Therefore, a balance of the degree of thermal isolation achieved vs. the volume of rover utilized is required to reach an acceptable design. The temperature differences between the controlled components and the rover structure vary from location to location so each gap has to be evaluated on a case-by-case basis to arrive at an optimal thickness. For every configuration and temperature difference, there is a critical thickness below which the heat transfer mechanism is dominated by simple gaseous thermal conduction. For larger gaps, the mechanism is dominated by natural convection. In general, convection leads to a poorer level of thermal isolation as compared to conduction. All these considerations play important roles in the optimization process. A three-step process was utilized to design this insulation. The first step is to come up with a simple, textbook based, closed-form equation assessment of gap thickness vs. resultant thermal isolation achieved. The second step is a more sophisticated numerical assessment using Computational Fluid Dynamics (CFD) software to investigate the effect of complicated geometries and temperature contours along them to arrive at the effective thermal isolation in a CO_2 atmosphere. The third step is to test samples of representative geometries in a CO_2 filled chamber to measure the thermal isolation achieved. The results of these assessments along with the consistency checks across these methods leads to the formulation of design guidelines for gap implementation within the rover geometry. Finally, based on the geometric and functional constraints within the real rover system, a detailed design that accommodates all these factors is arrived at. This paper will describe in detail this entire process, the results of these assessments and the final design that was implemented.

[1] Principal Thermal Engineer, Spacecraft Thermal Engineering Group
[2] Thermal Engineer, Thermal Hardware and Fluid Systems Engineering Group
[3] Thermal Engineer, Thermal Hardware and Fluid Systems Engineering Group
[4] Senior Thermal Engineer, Spacecraft Thermal Engineering Group

Nomenclature

AFT = *Allowable Flight Temperature*
BOL = *Beginning of Life*
CFC-11 = *Trichloromonofluoromethane (Refrigerant 11)*
CIPA = *Cruise Integrated Pump Assembly*
CHRS = *Cruise Heat Rejection System*
HRS = *Heat Rejection System*
JPL = *Jet Propulsion Laboratory*
MER = *Mars Exploration Rover*
MMRTG = *Multi Mission Radioisotope Thermoelectric Generator*
MPF = *Mars Pathfinder*
MPFL = *Mechanically Pumped Fluid Loop*
MSL = *Mars Science Laboratory*
MSLFT = *MSL Focused Technology Program*
NASA = *National Aeronautics and Space Administration*
PDT = *Pacific Design Technologies*
RAMP = *Rover Avionics Mounting Plate*
RIPA = *Rover Integrated Pump Assembly*
RHRS = *Rover Heat Rejection System*
WCC = *Worst Case Cold*
WCH = *Worst Case Hot*

I. Introduction

CRUISE CONFIGURATION – The mission follows the general design paradigm of the previous JPL rover missions to Mars (Mars Pathfinder, MPF[1,2,3,4,5] and Mars Exploration Rovers, MER[6,7]). The external configuration of the MSL spacecraft is similar to that of MPF and MER. However, at 4.5 meters, the diameter of the MSL spacecraft, is almost twice that of the MPF and MER spacecraft (2.6 m). MSL will feature a rover enclosed in an aero-shell for protection during entry and descent into the planet's atmosphere. A cruise stage will carry the lander and aero-shell enclosure from Earth to Mars and will separate from the Lander just prior to Entry, Descent and Landing (EDL). Figure 1 shows a rendering of the rover packed into the aero-shell enclosure with the Cruise Stage attached at the top.

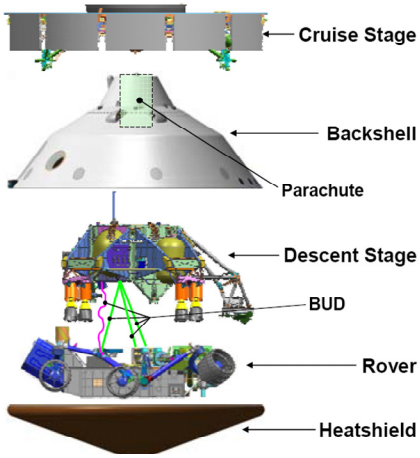

Figure 1. MSL Spacecraft.

The MMRTG is structurally attached to the rover and dissipates roughly 2000 W of waste heat and weighs approximately 40 kg. The descent stage, containing a propulsion system and avionics, is adjacent to the stowed rover. The cruise stage contains avionics, a propulsion system and the pumped fluid loop radiators.

SURFACE CONFIGURATION – The surface system consists of a large rover that is capable of traversing long distances on the Martian surface. Figure 2 shows the deployed rover with its integrated MMRTG. At roughly 850 kg, the MSL rover weighs almost five times that of MER rovers (~185 kg each).

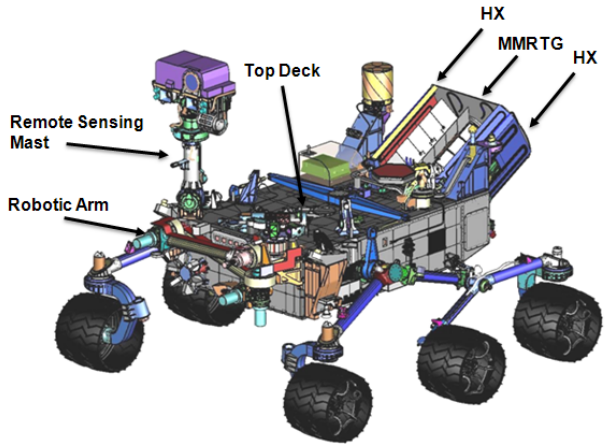

Figure 2. MSL Rover.

II. Rover Thermal Architecture

The MSL rover utilizes a mechanically pumped, single-phase fluid loop heat rejection system (HRS) to create the backbone for thermal control[8,9,10,11,12,13,14]. The fluid loop uses chlorofluorocarbon-11 (CFC-11) as the working fluid. Figure 3 shows the overall thermal architecture. The Rover HRS (RHRS) heat exchanger assemblies (hot and cold paltes) next to the MMRTG are shown in Figure 4.

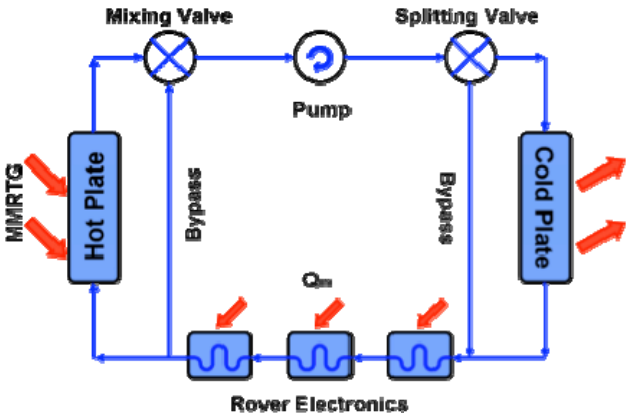

Figure 3. MSL HRS.

The overall system approach is to utilize this HRS architecture for the majority of the thermal control of the rover during Mars surface operations. The main impetus behind this approach is to utilize, as much as possible, the waste heat from the MMRTG during cold conditions, and to reject heat via HRS radiators during hot conditions.

The combination of MMRTG waste heat and HRS fluid loop greatly simplifies the rover thermal design in terms of the level of thermal isolation required to maintain the rover and payload at allowable temperatures during cold conditions. It also greatly improves the robustness of the design, decouples the mechanical design and configuration from the thermal design and reduces the level of testing required.

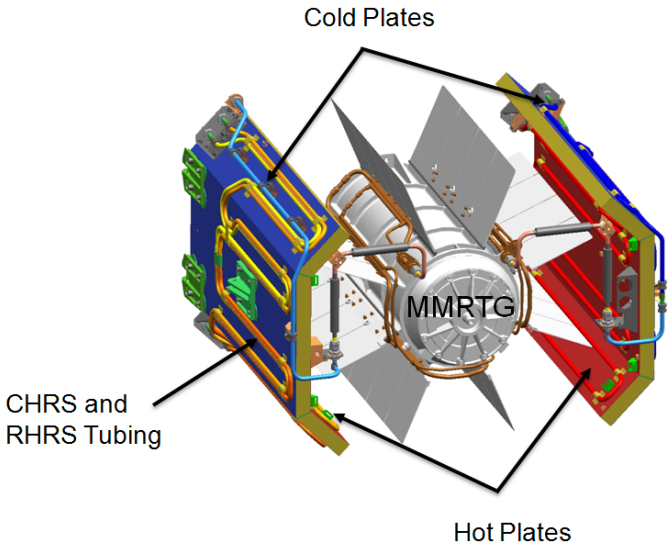

Figure 4. RHRS Heat Exchanger Assemblies, Red Facesheets-Hot Plates, Blue Facesheets-Cold Plates.

III. Usage of CO_2 Insulation for Conserving Heat on Mars

The key electronic components and instruments in the rover are mounted on a Rover Avionics Mounting Plate (RAMP) that has the HRS tubing attached to it. The routing of this tubing is done to strategically locate the tubing adjacent to the interfaces of all the components (avionics, instruments) that are mounted on the RAMP and thermally controlled by the HRS (Figure 5 shows view from back side of RAMP). The layout of the rover components on the RAMP is shown in Figure 6.

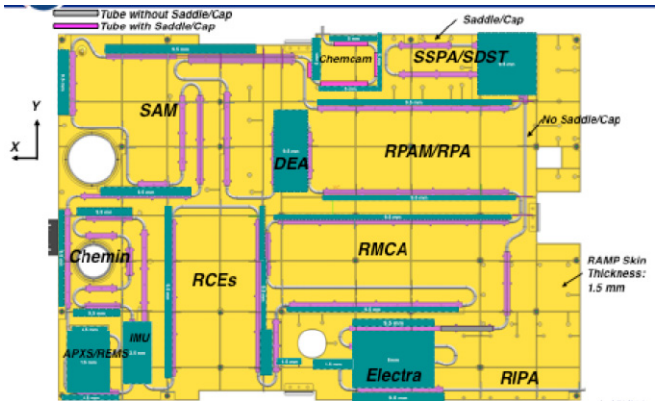

Figure 5: HRS Tubing Layout on RAMP

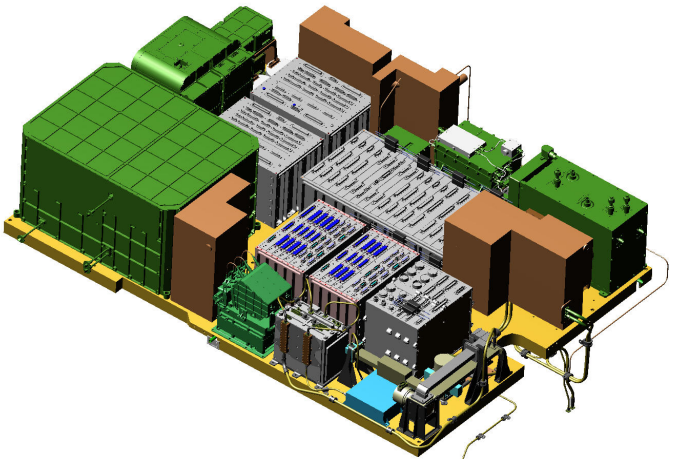

Figure 6: Rover components mounted on RAMP

To minimize heat loss from the RAMP, it is mechanically hung from the rover top deck via titanium supports, which have a small cross section area and long lengths to reduce their thermal conductance. A side view of this configuration is shown in Figure 7. The rover chassis (Figure 8), in turn, surrounds the entire assembly of the RAMP and top deck; the chassis has wheels, which drive the rover on the surface of Mars.

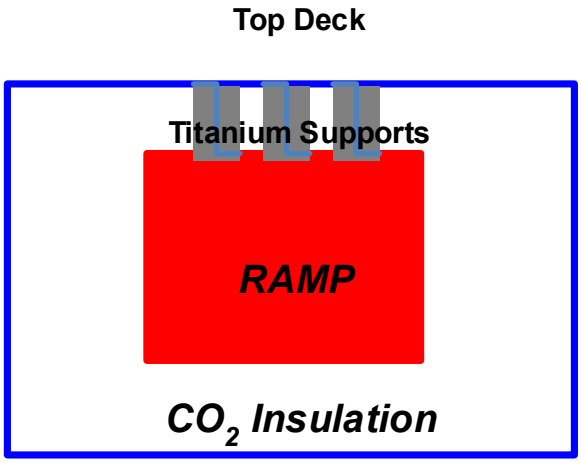

Figure 7. Side view of RAMP Supports.

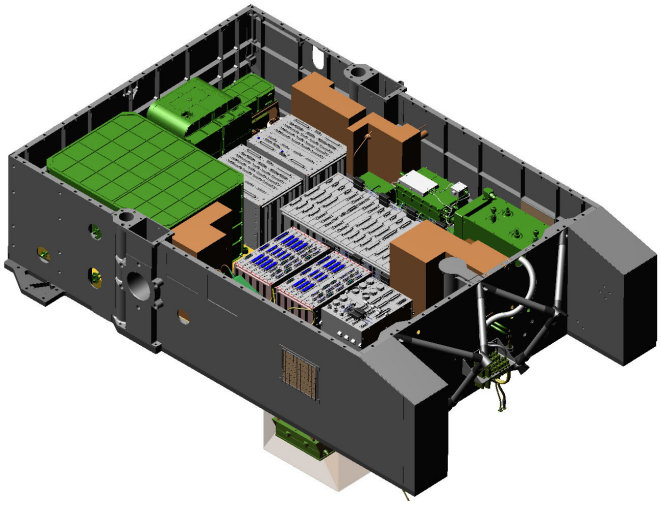

Figure 8. Rover chassis surrounding RAMP.

The total estimated heat loss of 150 W from the RAMP, in the coldest conditions, is comprised of four primary paths: CO_2 insulation, structural support, cable conduction and radiation. CO_2 insulation accounts for about a quarter of this total, hence is a significant factor for thermal control.

The thermal conductivity of CO_2 at 8 Torr varies from 0.01 W/m-K at -60°C, to 0.016 W/m-K at room temperature. Due to the low thermal conductivity of CO_2 gas, it serves as a natural (and "free") insulation to minimize heat loss from the thermally controlled components on the RAMP to the Mars atmosphere, ground and sky. Carefully designed gaps between the components and the chassis walls, the belly pan and between the RAMP and the top deck automatically get filled with ambient CO_2 upon landing on Mars due to vent holes in the chassis.

Larger gaps would improve the insulation but would also lead to less efficient use of the precious rover internal volume for installing components within the rover. This volume is very precious but so is the heat required to overcome the heat losses from the RAMP. So the primary tradeoff for designing these CO_2 gaps between the components on the RAMP and the surrounding chassis walls and top deck is geared towards minimizing the heat loss from these components (larger gaps) and minimizing the corresponding unused volume of the rover internal volume that is used as gaps to be filled by CO_2 once we arrive on Mars (smaller gaps). The research described in this paper was conducted to find the heat loss characteristics of gaps of various thicknesses to allow us to find this optimal balance.

IV. Parameters That Affect Heat Loss Via CO_2 Gas Gaps

For a given heat flow area, the heat loss via gas gaps depend on several factors:

- Gap thickness: heat loss decreases with increasing gap thickness
- Orientation: Vertical gaps tend to lose more heat
- Temperature difference: Larger temperature differences lead to larger losses
- Temperature of gaps: Thermal conductivity of CO_2 increases with temperature
- Aspect ratios of gaps: Larger area to height ratios tend to reduce edge effects and be less effective in insulating

Since the RAMP has boxes that have different heights and shapes, and since the RAMP and the surrounding chassis experience varying temperatures on Mars, all of the above parameters come into play in the optimization of the design of these gaps. Therefore, both the analytical and experimental assessment varied these parameters to fully capture their impact on their optimization.

V. Process for Assessing CO_2 Gap Thermal Characteristics

A three-step approach, in the following order, was taken to arrive at the optimal gaps. The first approach was to use standard textbook based closed form equations to characterize heat losses. The second approach was the CFD evaluation. And the third and last approach was to set up an experiment in a test chamber to carefully measure the heat loss for the chosen combinations.

This turned out to be a quick and efficient way to arrive at the optimal configurations because it progressively filtered out non-optimal gaps to reduce the number of expensive CFD runs by using the text book equations to get a 1st order feel for the right set of parameters. Similarly, the CFD runs filtered out unnecessary and expensive test conditions.

VI. Text Book Based Assessment

The thermal conductivity of CO_2 gas (Figure 9) is strongly dependent on temperature and is independent of pressure over the range of interest. So for pure conduction (no convection), a given ΔT, k and L, the heat loss is inversely proportional to L as shown in Figure 10.

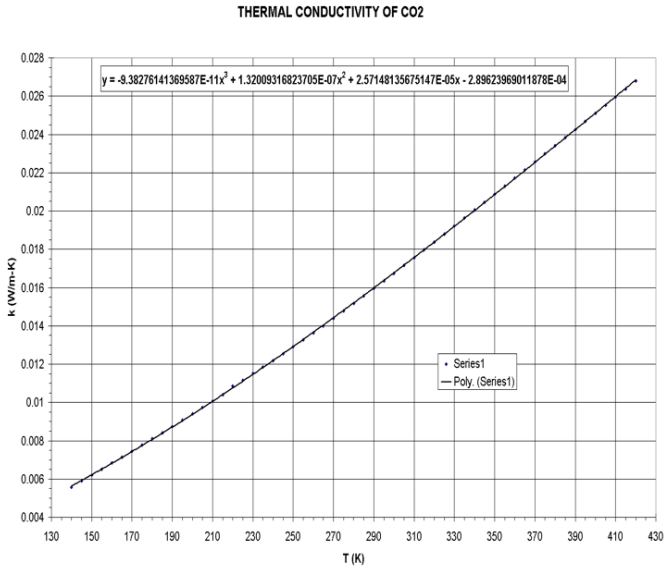

Figure 9. Thermal Conductivity of CO_2 gas.

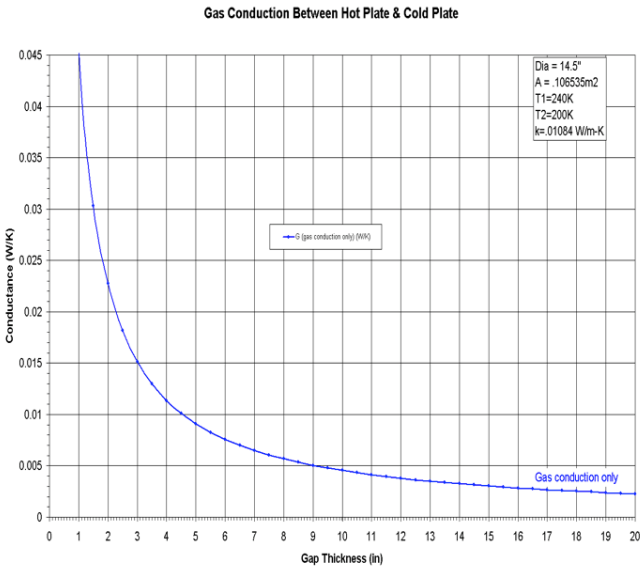

Figure 10. Heat conductance with pure conduction in CO_2 gas.

However, when both conduction and convection are present, the following closed form equations from Holland's paper[15] were used to make the "text book" assessments:

For horizontal parallel plates (hot plate on the bottom):

- $Nu = 1 + 1.44\,[1 - (1708 / Ra)] + [(Ra / 5830)^{(1/3)} - 1]$
- If either term in square brackets above is negative, it must be set to zero.

For vertical parallel plates:

- $Nu = \max\,\{Nu_1, Nu_2, Nu_3\}$
- $Nu_1 = 0.0605(Ra)^{(1/3)}$
- $Nu_2 = \{1 + [(0.104(Ra)^{0.293}) / (1 + (6310/ Ra)^{1.36})]^3\}^{(1/3)}$
- $Nu_3 = 0.242\,[Ra / (H/L)]^{0.272}$

The following nomenclature applies to the above equations:

G – conductance [W/K]
h – convection coefficient [W/m2-K]
A – area [m^2]
k – conductivity [W/m-K]
L – plate separation [m]
Ra – Raleigh number [--]
Nu – Nusselt number [--]
Gr – Grashof Number [--]
T_{avg} – Average temperature [K]
ΔT – delta temperature [K]
Pr – Prandtl number [--]
ν - kinematic viscosity [m^2/s]
H – plate diameter [m]
g – 9.81 m/s^2 for Earth gravity, 3.68 m/s^2 for Mars gravity
G = hA
h = (Nu)(k)/(L)
$Ra = GrPr = (1/T_{avg})(\Delta T)(g)(L^3)(Pr) / (\nu^2)$

Using the above correlations, Figure 11 shows the thermal conductance for a representative set of parameters, including area of heat flow, heat source (-30 ^{o}C) and sink (-70^{o}C) temperatures, for variable gap thickness for both Earth and Mars gravitational accelerations, and for both horizontal and vertical orientations. Some key observations can be made as follows:

- The magnitude of convection is less on Mars than on Earth – Earth test data will be conservative
- Convection begins at larger gap thicknesses on Mars than on Earth - Earth test data will be conservative
- For gap thicknesses less than roughly 63 mm (2.5”), there is gas conduction only (no convection) - pure conduction is a good assumption for small gaps
- Gas conduction of a 3.8 cm (1.5”) thick gap is greater than the conduction + convection of any larger gap size - assuming 3.8 cm (1.5”) of pure conduction is conservative for larger gaps.
- Vertical and horizontal convection is similar in magnitude for gap thicknesses less than roughly 20.3 cm (8”) - test data in horizontal orientation is roughly applicable to vertical orientation

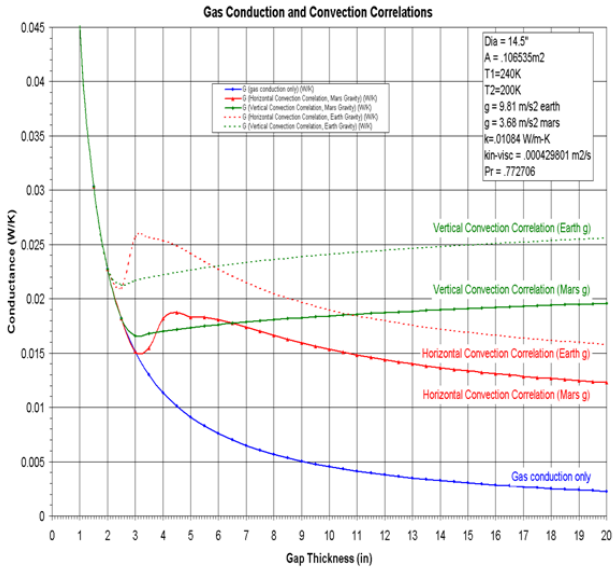

Figure 11. Conduction and convection correlations.

VII. CFD Assessment

Since the simple equations are for broad-based use for a variety of conditions and geometries, a more accurate scheme to analytically make the heat loss estimates for various gas gaps, orientations and operating parameters, was undertaken using CFD analysis. The geometry and operating conditions of the expected test article was simulated in the analyses. CFD is particularly useful for accounting for edge effects at the radial interface between main test article (parallel plates) and the rest of the test chamber gas volume. The edge effects can locally distort the convective flow field at the radial edges, which is ignored in the simple closed form equations, but can be simulated and understood in the CFD analyses.

Horizontal gaps varying from 2.5 cm (1”) to 50 cm (20”) were simulated. Vertical gaps of 5 cm (2”) and 25 cm (10”) were simulated. The heated plate was held as a boundary at -30^{o}C, while the cooled plate was held at -80^{o}C.

Sample snapshots of the horizontal plate model runs are shown in Figures 12 and 13. It is evident that < 3.8 cm (1.5”) gaps no convective cells form within the parallel plates and pure conduction is a good assumption. For larger gaps, say 12.7 cm (5”), significant convection can be observed from the CFD runs.

For a vertical plate Figure 14 shows the snapshot for a 5 cm (2”) gap and hardly any convection is observed, but large gaps (Figure 15), say 25 cm (10”), significant convection is observed.

The process of computing the thermal conductance in the CFD runs was to use a fixed heater input in the heated plate and the computed hot plate temperature (for a fixed cold plate temperature) determines the thermal conductance across the gas gap.

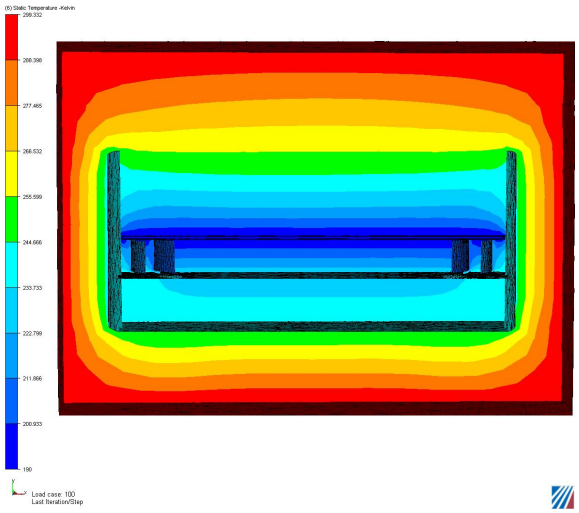

Figure 12. CFD run for horizontal plate with 3.8 cm (1.5") gap.

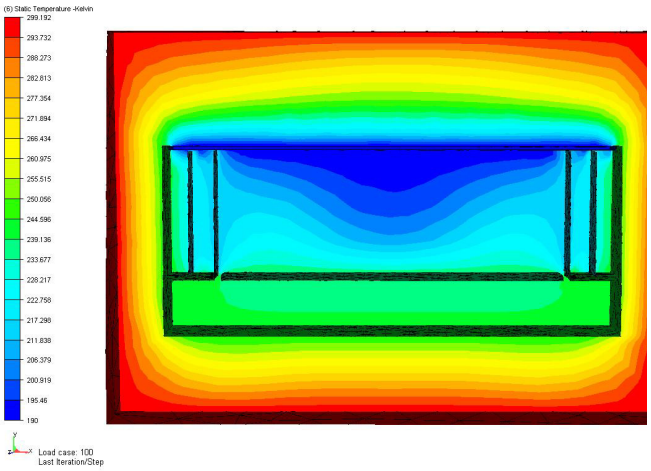

Figure 13. CFD run for horizontal plate with 12.7 cm (5") gap.

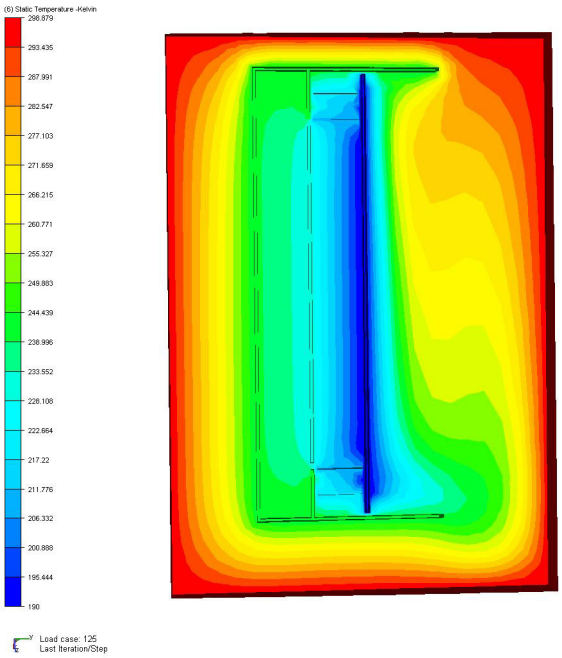

Figure 14. CFD run for vertical plate with 5 cm (2") gap.

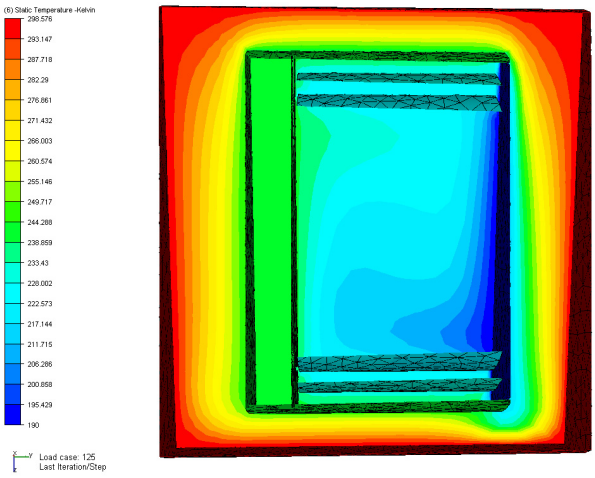

Figure 15. CFD run for vertical plate with 25 cm (10") gap.

The results of the CFD runs are shown in Figure 16, where the thermal conductance is plotted as a function of the gap thickness (for Earth g to simulate the test setup conditions), for a horizontal orientation. Also plotted are corresponding text book based predictions for horizontal and vertical orientations, as well as simple conduction only predictions.

Some key observations are:

- For gaps < 3.8 cm (1.5") all correlations (text book & CFD) collapse into a single value based on pure conduction only
- For horizontal gaps larger than 3.8 cm (1.5"), CFD runs tend to predict higher conductances than those from the textbook equations
- At gaps > ~5 cm (2"), CFD based conductances bottom out (they don't change with larger thicknesses)
- There is negligible convection at small gap thicknesses <5 cm (2.5")

- The CFD results show that the transition from conduction to convection at increasing gap thicknesses is even more gradual and benign than those predicted by text book based equations

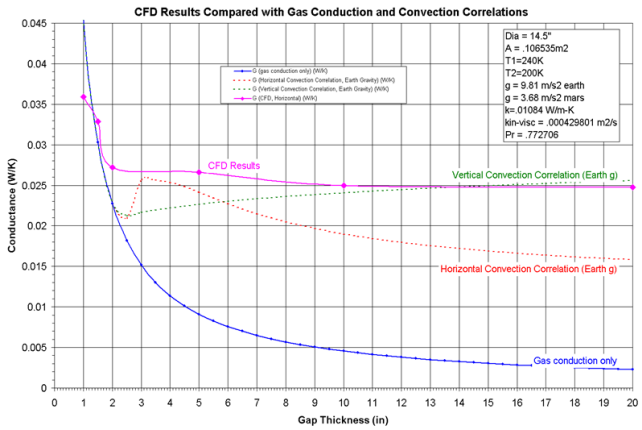

Figure 16. CFD results and convection correlations.

VIII. Test Approach

The basic test approach was to use two parallel plates constructed of aluminum sheets 37 cm (14.5") in diameter in a bell jar, with a well-controlled gap between them. This gap would then represent the gas gap under investigation for that particular test case. One plate (hot plate) is heated by an film heater. The other plate (cold plate) is cooled by a cooling coil with cold gas flowing through it. The two plates are isolated from each other and the bell jar walls by G-10 isolators. All surfaces of the parallel plates are covered with low emissivity (gold) plate to minimize radiation heat transfer between the plates to improve the fidelity of the data (gas conduction/convection to dominate radiation). The bell jar is filled with CO_2 and N_2 gases at 8 Torr to simulate the Martian atmosphere as well as solar thermal vacuum test conditons (for system thermal testing of rover in a simulation chamber using N_2).

To minimize test set up induced edge effects, an annular guard heater plate is employed around the cold plates. To maximize the data resolution, a guard heater plate is also employed between the cold plate and the bell jar walls (to only allow heat transfer between the hot and cold plates and minimize any heat transfer between the cold plate and the bell jar). Edges of the cold and hot plates were sealed with Goldized-Kapton tape to prevent convection cells from going around edges of these plates.

Tare values of heat transfer are measured between the hot and cold plates in a vacuum to compute the radiation and conduction (via mechanical supports). This value is subtracted out of the total heat flow in the presence of gaseous CO_2 (or N_2) to arrive at only the conduction/convection heat transfer via the gas. A schematic of the test setup is shown in Figures 17 & 18. Photos of the actual test setup are shown in Figure 19.

The test cases employed horizontal gas gaps of 3.8 cm (1.5"), 5 cm (2"), 7.6 cm (3"), 10 cm (4") and 12.7 cm (5") thicknesses. Due to the size and shape of the test article in comparison to the test chamber, vertical orientations were not feasible in this test.

The results of the test are shown in Figure 20. The thermal conductance of the gas gap vs. gap thickness is plotted. Along with the test measurements, the corresponding results of analytical estimates of this conductance are presented for comparison with test data. The analytical results pertain to both text book based equations (pure conduction and conduction plus convection) as well as the CFD results. Since the test was done in 1g with CO_2, only results pertaining to these conditions are compared in this plot.

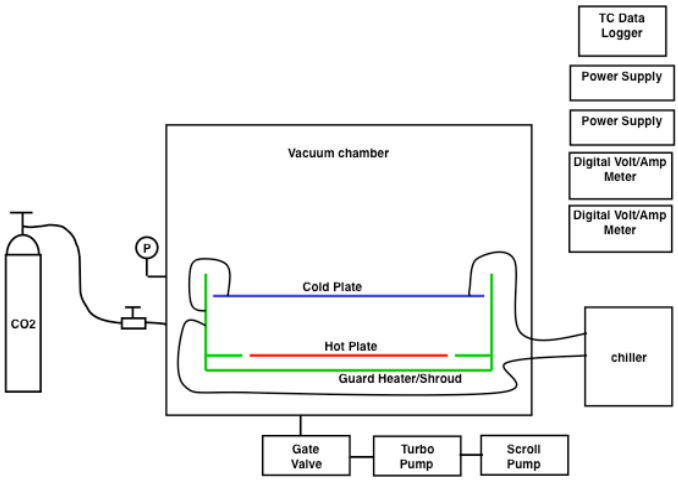

Figure 17. Test setup schematic.

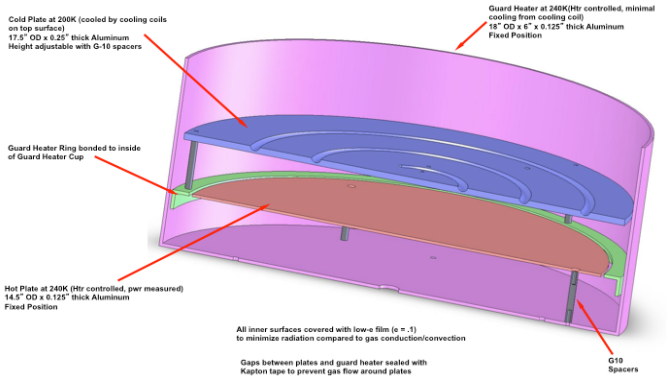

Figure 18. Test hardware configuration.

Figure 19. Photos of test hardware.

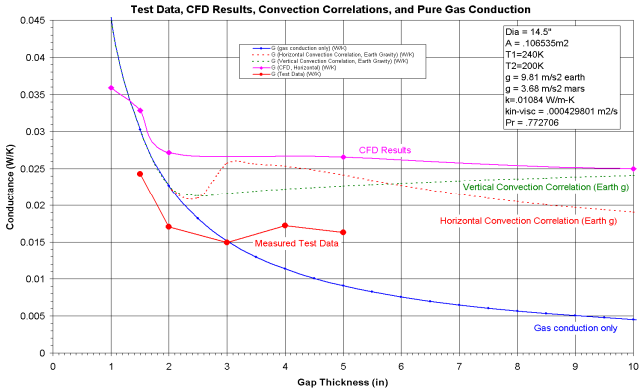

Figure 20. Test data, CFD, and textbook correlations.

The key conclusions from these tests are shown below:

- Test results showed generally greater heat loss than pure gas conduction calculations at larger gap thicknesses, but consistently less heat loss than predicted by CFD or convection correlations - results show that convection correlations are conservative compared to test data.

- The onset of convection occurred at a greater gap thickness ~7.6 cm (3") than predicted by convection correlations ~6.4 cm (2.5") - convection correlations are conservative compared to test data.

- No convection scenario was found at larger gap thickness that produces more heat transfer than a simple conservative assumption of pure gas conduction with a 3.8 cm (1.5") thick gas gap.

- The general trend of the data was consistent with the trends predicted by CFD, convection correlations, and pure conduction calculations.

- All of the test results were positive when compared to conservative rover thermal model assumptions. The test results further increased confidence in the thermal design assumptions.

IX. OVERALL IMPLEMENTATION OF GAS GAPS BASED ON ANALYTICAL & TEST BASED ASSESSMENTS

- Conservative allocations were made for minimum gas gap thicknesses between the RAMP component envelopes and the adjacent rover chassis walls: 7.6 cm (3") top, 5 cm (2") bottom, and 3.8 cm (1.5") sides. These were designated to be stay out zones to ensure that no components violate these thermal isolation gaps.
- Since the actual configuration has components creating a skyscraper like envelope with varying gaps between the the components and the chassis walls, in general, the implementation of these designed gaps was achieved by prescribing a space between the component envelopes and the adjoining cold walls (chassis or top deck) to be at least a thickness equal to the minimum gap required, based on the information provided by the test data.
- For the top of the rover, the primary driver for the 7.6 cm (3") gap was the spacing required to mechanically support the RAMP from the top deck, while at the same time being thermally isolative via these supports (trade-off between structural and thermal properties of the mechanical supports). Per the test data (Figure 20), usage of a pure conduction assumption to compute the heat loss was judged to be adequate and no baffles were used to break this gap into smaller ones.
- For the sides of the rover, there is negligible convection because the minimum gap is 3.8 cm (1.5") thick. Convection correlations, CFD analysis and testing agree that there is no convection for gaps less than 6.4 cm (2.5") thick. For areas where the side gap is greater than 3.8 cm (1.5") thick, correlations and CFD agree that the magnitude of convection plus conduction at larger gaps is still less than pure gas conduction at 3.8 cm (1.5") thick, hence a pure conduction assumption was utilized to compute the heat loss via the sides.

- For the bottom of the rover, a minimum of 5 cm (2") gap was utilized, and based on test data (Figure 20), a pure conduction assumption was judged to be adequate to compute the heat loss from the bottom of the RAMP component envelopes for areas where the side gap is greater than 5 cm (2") thick - similar to how the rover sides were handled. Additionally, for the bottom of the rover, there is negligible convection because the cold belly-pan is below the warm RAMP components.
- Hence overall, in the rover thermal models, heat loss is calculated based on gas conduction only, which will be conservative in estimating the heat loss, based on the explanations provided above.

X. Conclusions

This paper presented an overview of the design, analysis, testing and implementation of CO_2 gaps as insulation for the components of the Mars Science Laboratory rover. Recent testing of this rover in a solar thermal gaseous environment to simulate the conditions on the Martian surface demonstrated that this insulation system is robust and exhibits substantial margin against its design requirements. The design approach and trade offs presented in this paper provide the necessary tools for utilizing this type of insulation system in future interplanetary missions in their current or extrapolated forms.

Acknowledgments

The work described in this paper was performed at the Jet Propulsion Laboratory, California Institute of Technology, under a contract with the National Aeronautics and Space Administration. The authors wish to acknowledge the many engineers and scientists collaboratively working on the Mars Science Laboratory project, of which, the thermal subsystem is a part of the greater whole.

References

[1]Bhandari, P., Birur, G.C., and Gram, M.B., "Mechanical Pumped Cooling Loop for Spacecraft Thermal Control," SAE Technical Paper No. 961488, 26th International Conference on Environmental Systems, Monterey, California, July 8-11, 1996.

[2]Birur, G.C., Bhandari, P., Gram, M.B., and Durkee, J., "Integrated Pump Assembly- An Active Cooling System for Mars Pathfinder Thermal Control," SAE Technical Paper No. 961489, 26th International Conference on Environmental Systems, Monterey, California, July 8-11, 1996.

[3]Birur, G. and P. Bhandari, "Mars Pathfinder Active Thermal Control System: Ground and Flight Performance of a Mechanically Pumped Loop," Paper No AIAA-97-2469, 32nd Thermophysics Conference, Atlanta, GA, June 23-25, 1997.

[4]Birur, G.C. and Bhandari, P., "Mars Pathfinder Active Heat Rejection System: Successful Flight Demonstration of a Mechanically Pumped Cooling Loop," SAE Technical Paper No. 981684, 28th international Conference on Environmental Systems, Danvers, Massachusetts, July 13-16, 1998.

[5]Lam, L, Birur, G., and Bhandari, P., "Pumped Fluid Loops," *Satellite Thermal Control Handbook (2nd edition)*, Ed. D. Gilmore, Aerospace Corporation, El Segundo, California, 2002.

[6]Ganapathi, G., Birur, G., Tsuyuki, G., and Krylo, R., "Active Heat Rejection System on Mars Exploration Rover – Design Changes from Mars Pathfinder", Space Technology Applications International Forum 2003, Albuquerque, NM, February 2-5, 2003.

[7]Tsuyuki,G. ,Ganapathi,G. ,Bame,D. ,Patzold, J., Fisher, R., and Theriault, L., "The Hardware Challenges for the Mars Exploration Rover Heat Rejection System," AIP Conference Proceedings, Vol. 699(1), pp. 59-70. February 2004.

[8]Bhandari, P., Birur, G., Pauken, M., Paris, A., Novak, K., Prina, M., Ramirez, B., and Bame, D., "Mars Science Laboratory Thermal Control Architecture," SAE 2005-01-2828, 35th International Conference on Environmental Systems, Rome, Italy, July 2005.

[9]Birur, G., Bhandari, P., Prina, M., Bame, D., Yavrouian, A., and Plett, G., "Mechanically Pumped Fluid Loop Technologies for Thermal Control of Future Mars Rovers," SAE 2006-01-2035, 36th International Conference on Environmental Systems, Norfolk, Virginia, July 2006.

[10]Birur, G.C., Prina, M, Bhandari, P, et al, "Development of Passively Actuated Thermal Control Valves for Passive Thermal Control of Mechanically Pumped Single Phase Fluid Loops for Space Applications," 38th International Conference on Environmental Systems, San Francisco, California, June 29-July 2, 2008

[11]Bhandari, P, et al, "Mars Science Laboratory Rover Thermal Control Using a Mechanically Pumped Fluid Loop", Space Technology & Applications International Forum (STAIF-2006), March, 2006

[12]Bhandari, P, "Mechanically Pumped Fluid Loops for Spacecraft Thermal Control, Past , Present and Future", 15th Annual Thermal & Fluid Analysis Workshop (TFAWS), 2004, Pasadena, CA

[13]Bhandari, P., Birur, G.C., et al, "Mechanically Pumped Fluid Loop Heat Rejection & Recovery Systems For Thermal Control on Martian Surface – Case Study of The Mars Science Laboratory," 36th International Conference on Environmental Systems, Norfolk, Virginia, July 2006.

[14]Paris, A.D, et al, “Thermal Design of the Mars Science Laboratory Powered Descent Vehicle,” 38th International Conference on Environmental Systems, San Francisco, California, June 29-July 2, 2008
[15]Hollands, et al, "Free Convective Heat Transfer Across Inclined Air Layers", Journal of Heat Transfer, Transactions of the ASME, vol. 98(2), pg. 189-193, 1976.